https://doi.org/10.1007/s11467-024-1414-7

RESEARCH ARTICLE

Stable alkali halide vapor assisted chemical vapor deposition of 2D $HfSe_2$ templates and controllable oxidation of its heterostructures

Wenlong Chu[1], Xilong Zhou[1], Ze Wang[2], Xiulian Fan[1], Xuehao Guo[1,3], Cheng Li[1], Jianling Yue[2], Fangping Ouyang[1,2,3], Jiong Zhao[4], Yu Zhou[1,2,†]

[1]School of Physics, Hunan Key Laboratory of Nanophotonics and Devices, Central South University,
Changsha 410083, China
[2]State Key Laboratory of Powder Metallurgy, Central South University, Changsha 410083, China
[3]School of Physical Science and Technology, Xinjiang University, Urumqi 830046, China
[4]Department of Applied Physics, The Hong Kong Polytechnic University, Kowloon, Hong Kong, China
Corresponding author. E-mail: †yu.zhou@csu.edu.cn

Received April 1, 2024; accepted April 20, 2024

Supporting Information

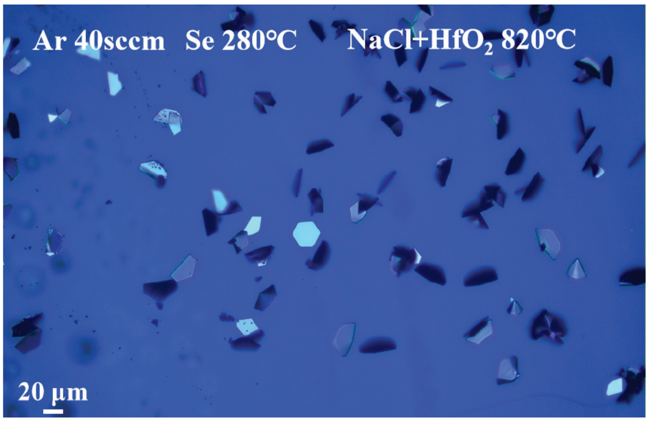

Fig. S1 Optical image of typical 2D $HfSe_2$ random vertical nanoflakes by the mixed NaCl and HfO_2 powders.

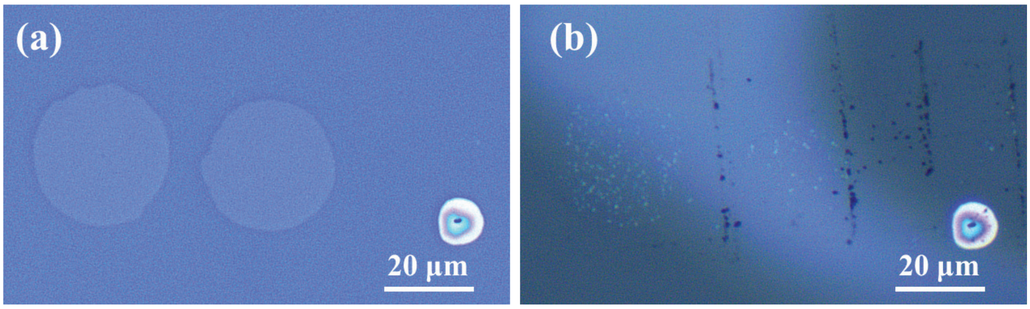

Fig. S2 (a) Optical image of $HfSe_2$ when just removed from the tube furnace. **(b)** Optical image of $HfSe_2$ after AFM test (after about 30 minutes), in which the samples disappeared.

Due to the environmental instability of $HfSe_2$, extremely thin $HfSe_2$ nanosheets have been largely degraded by exposure to air for about 30 min.

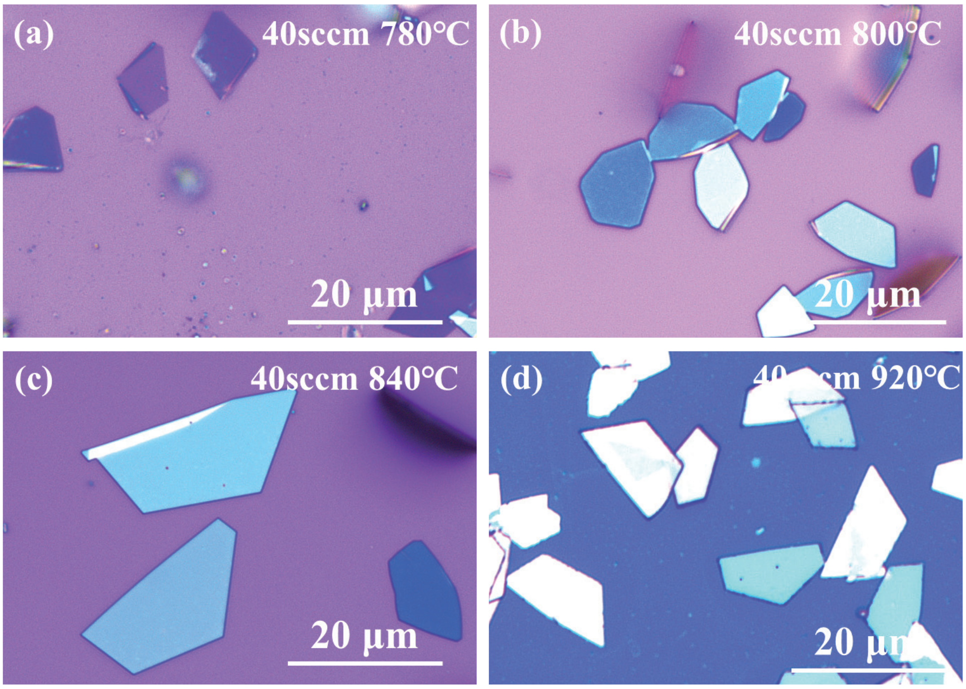

Fig. S3 (a–d) Optical images of $HfSe_2$ nanosheets grown on mica substrates at different center temperatures: 780°C, 800°C, 840°C, and 920°C, respectively, all with an argon flow rate of 40 sccm and Se temperature of 290 °C.

A higher nucleation density and randomly vertical growth of 2D $HfSe_2$ nanosheets on SiO_2/Si substrates were demonstrated, which may be due to the different nucleation and migration barriers caused by unsaturated dangling bonds on the SiO_2 surface. Moreover, the samples on SiO_2/Si substrates tend not to have regular hexagonal shapes and are much thicker than the samples on mica substrates. This can be attributed to the surface inertness of the mica substrate and the smaller migration barrier that promotes the rapid lateral growth of 2D nanosheets.

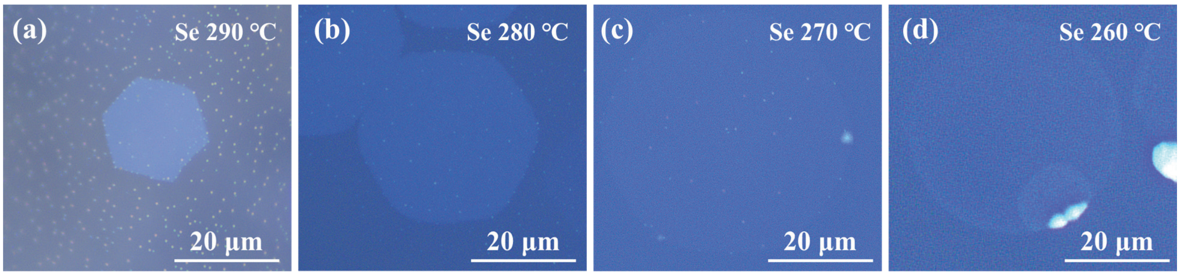

Fig. S4 Morphological evolution of $HfSe_2$ nanosheets from hexagons to circles. **(a, b)** Optical images of $HfSe_2$ nanosheets obtained on mica substrates by varying the heating temperatures of 290°C, 280°C, 270°C, and 260°C for Se; the rest of the growth conditions were a central growth temperature of 780°C, an argon flow rate of 30 sccm, and a holding time of 10 min.

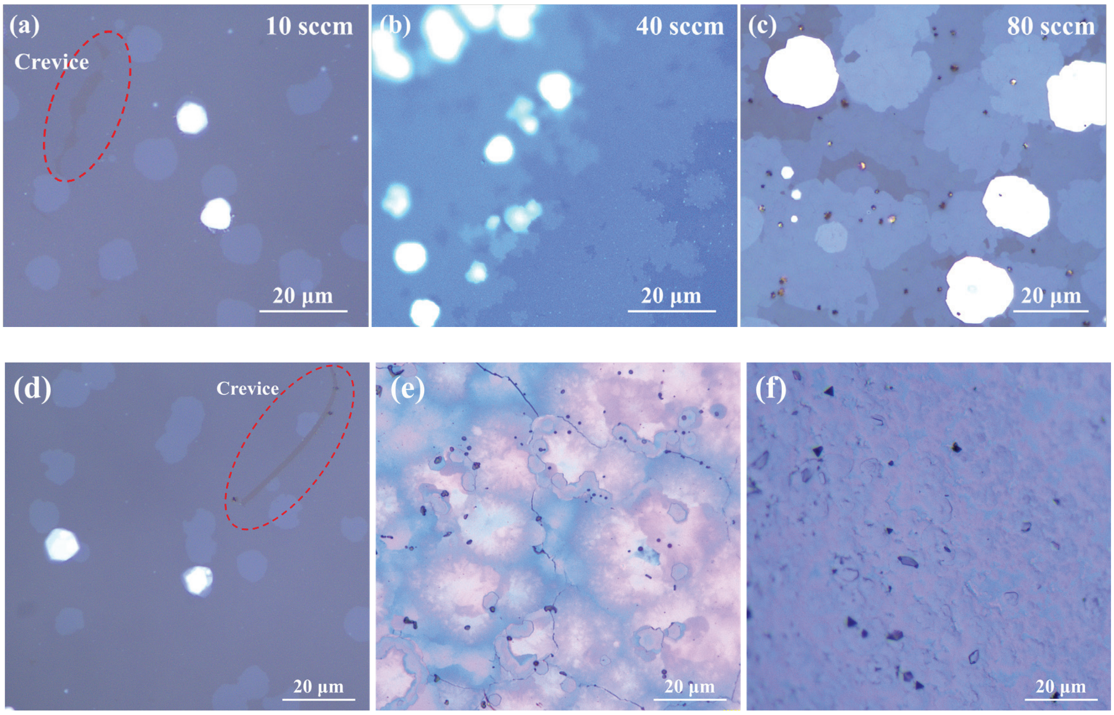

Fig. S5 A small range of HfSe$_2$ films with different thicknesses. **(a–c)** Optical images of HfSe$_2$ nanosheets obtained on mica substrates by varying the flow rate of argon 10 sccm, 40 sccm, and 80 sccm; the rest of the growth conditions were the central growth temperature of 860°C, the heating temperature of Se of 300°C, and the holding time of 10 min. **(d–f)** Optical images of HfSe$_2$ nanosheets obtained on mica substrates by controlling the flow rate of argon at a constant 10 sccm and varying the central growth temperatures of 840°C, 890°C, and 950°C; the rest of the growth conditions: heating temperature of Se at 300°C, holding time 10 min.

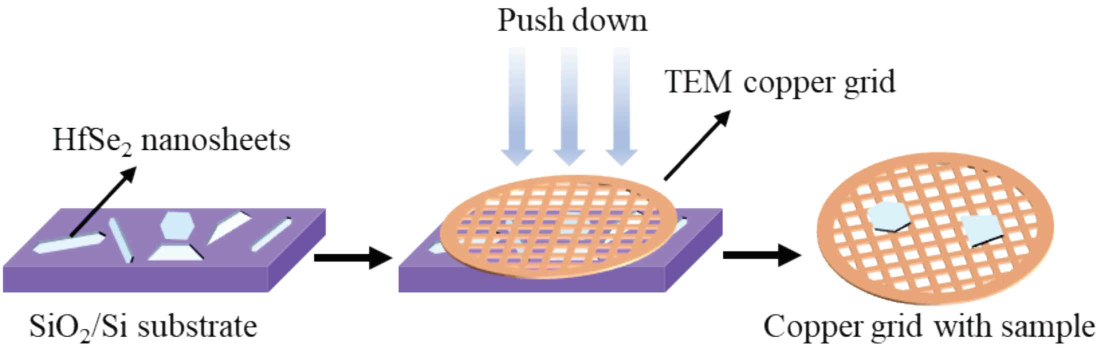

Fig. S6 Sample transfer on TEM copper grid.

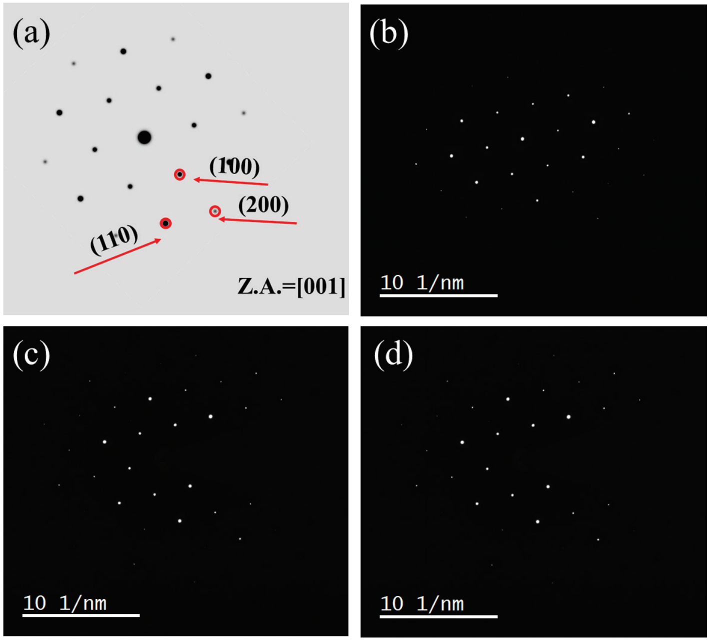

Fig. S7 (a) Electron diffraction simulated by Single Crystal software and its corresponding crystal planes. **(b–d)** Selected-area electron diffraction from different regions on the same $HfSe_2$ nanosheet.

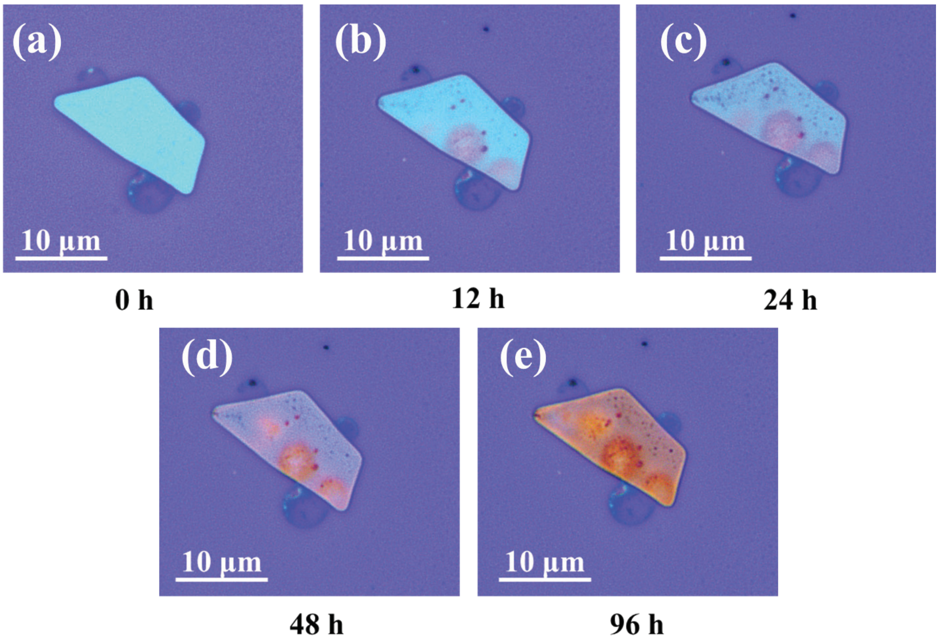

0 h **12 h** **24 h**

48 h **96 h**

Fig. S8 (a–e) Optical images of ~40 nm thick $HfSe_2$ nanosheets naturally oxidized in air for various times.

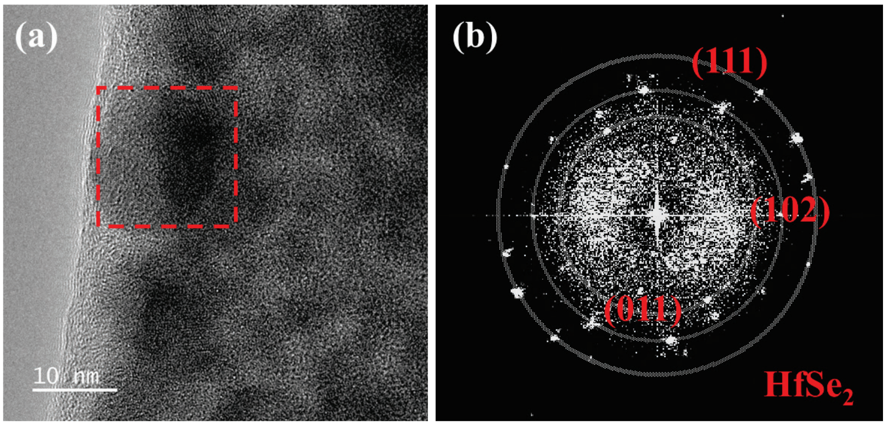

Fig. S9 (a, b) FFT images of different regions on high-resolution TEM images of oxidized HfSe$_2$ nanosheets.

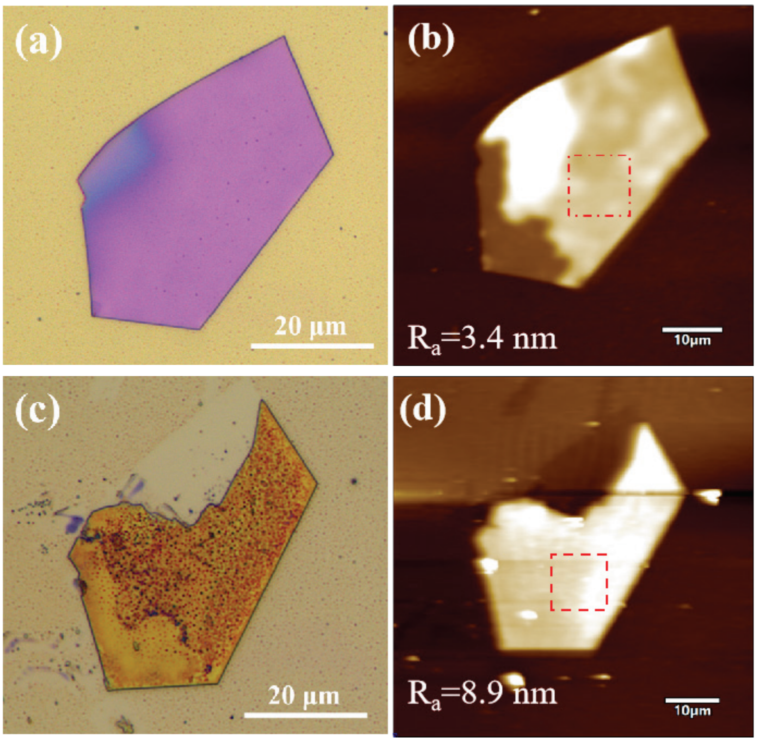

Fig. S10 (a, c) Optical comparison of HfSe$_2$ nanosheets before and after oxidation. **(b, d)** Surface roughness changes of HfSe$_2$ nanosheets before and after oxidation.

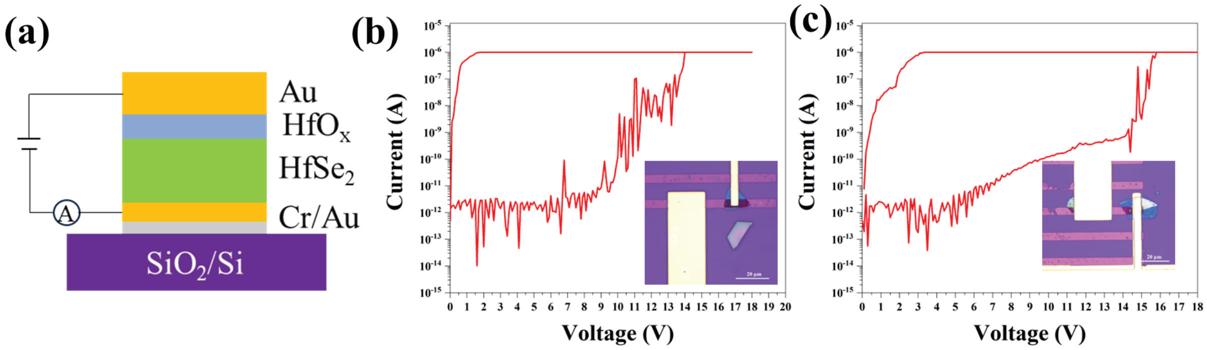

Fig. S11 (a) Schematic structure of an HfO$_2$–HfSe$_2$ memristor with both upper and lower electrodes of inert metal Au. **(b, c)** Typical *I*–*V* switching curves of three different HfO$_2$-HfSe$_2$ memristor devices.